

Exploring DeshuffleGANs in Self-Supervised Generative Adversarial Networks

Gulcin Baykal^{a,*}, Furkan Ozcelik^a, Gozde Unal^a

^a*Istanbul Technical University, Istanbul, Turkey*

Abstract

Generative Adversarial Networks (GANs) have become the most used network models towards solving the problem of image generation. In recent years, self-supervised GANs are proposed to aid stabilized GAN training without the catastrophic forgetting problem and to improve the image generation quality without the need for the class labels of the data. However, the generalizability of the self-supervision tasks on different GAN architectures is not studied before. To that end, we extensively analyze the contribution of the deshuffling task of DeshuffleGANs in the generalizability context. We assign the deshuffling task to two different GAN discriminators and study the effects of the deshuffling on both architectures. We also evaluate the performance of DeshuffleGANs on various datasets that are mostly used in GAN benchmarks: LSUN-Bedroom, LSUN-Church, and CelebA-HQ. We show that the DeshuffleGAN obtains the best FID results for LSUN datasets compared to the other self-supervised GANs. Furthermore, we compare the deshuffling with the rotation prediction that is firstly deployed to the GAN training and demonstrate that its contribution exceeds the rotation prediction. Lastly, we show the contribution of the self-supervision tasks to the GAN training on loss landscape and present that the effects of the self-supervision tasks may not be cooperative to the adversarial training in some settings. Our code can be found at

*Corresponding author

Email addresses: baykalg@itu.edu.tr (Gulcin Baykal), ozcelikfu@itu.edu.tr (Furkan Ozcelik), gozde.unal@itu.edu.tr (Gozde Unal)

<https://github.com/gulcinbaykal/DeshuffleGAN>.

Keywords: Self-Supervised Generative Adversarial Networks, Generative Adversarial Networks, Self-Supervised Learning, DeshuffleGANs, Deshuffling

1. Introduction

Generative Adversarial Networks (GANs) [1] followed and surpassed the pioneering Autoencoders [2] in employing deep neural networks (DNNs) for image generation with a certain quality in mimicking a desired data distribution. The main objectives of the image generation problem can be summarized as: generating high-quality images; generating diverse images; and achieving training stability [3]. Numerous GAN variants attempt at producing photo-realistic image generations while the latter are desired to vary and capture a considerable amount of different modes in the real data distribution.

The GAN model's ability to learn the structures and the semantics of the data improves the quality of the generations synthesized by the generator of the model. The generator part of the GAN is trained to decode vectors from a latent space where the space has a normal distribution onto a 2D image space, which is desired to have a data distribution similar to the real input data distribution. As the standard training mechanism of the GANs proposed in [1] needs additional guidance in order to support the generator for synthesizing high-quality images that capture the real data distribution, typically, the capacity of the discriminator part of the GAN is enhanced to provide this guidance.

The discriminator of the GAN model is trained to distinguish between the real samples of the original data and the fake samples of the generated data in that it may supervise the generator to produce more realistic images by the meaningful feedback it provides. The increased representation differentiating capacity of the discriminator introduces an enriched representation of the real data whereas the enhancement of the discriminator is attained by auxiliary signals and tasks.

Following the unconditional GAN model, which is described above, condi-

tional GAN models are proposed in conditional image generation where initially, the generations are conditioned on class labels. The conditional GAN makes use of the auxiliary signals of the labels in training, whereas the unconditional GAN utilizes the real/fake (r/f) information of the data as its only supervisory signal. Benefiting from the auxiliary signals can help to optimize the training of the GANs while it supports the generator to produce high-quality images. Labels for the input images are typically represented as vectors. Odena et al. [4] utilize the label vectors directly while Miyato et al. [5] project the label vectors instead of concatenation. The incorporation of the auxiliary signals into the adversarial training improves the stability and the quality of the class conditional image generations. In InfoGAN [6] and ACGAN [7], the discriminator tries to predict the class labels as the auxiliary task which enhances the representation capacity of the discriminator.

As the utilization of class labels as auxiliary signals and the enhancement of the discriminator with the auxiliary tasks improve the training stability and image generation quality of the GANs, the choice of the auxiliary task deserves additional attention. Since the auxiliary signals are attained by the labels of the datasets, training with the unlabeled datasets used as benchmarks in GANs cannot take the advantage of the additional supervisory signals. As the organization of large and diverse datasets with labels requires time and human resources which are expensive to have, benefiting from the datasets, which already vary and are large in numbers but do not have any labels, would support the image generations from different domains except the well-known ImageNet [8] and CIFAR [9] datasets with labels. As a remedy, a recent framework, known as the *self-supervised learning* can be utilized for compounding self-supervision tasks on unlabeled datasets to the GAN training as auxiliary signals in order to enhance the capacity of the discriminator at no computation and human resource cost.

To deploy the self-supervised learning into GANs, Chen et al. [10] proposed the first self-supervised GAN, the SS-GAN, with the auxiliary task of predicting the rotation angles of the input images for the discriminator. In [10], an improve-

ment in training stability is shown by the enhancement of the discriminator’s representation power in a way that overcomes the catastrophic forgetting problem to a certain degree [11]. In addition to the stability, it is shown on different benchmarks that [10] can catch up the performance of conditional GANs without benefiting the labeled data and even in some settings, outperforms them. Although the addition of the rotation prediction task improves the performance of GAN training, the effects of the other self-supervision tasks should be also analyzed in order to evaluate the corresponding potential improvements.

Tran et al. [12] study the effects of deploying self-supervision to GANs in the learning of the generator and enhances the self-supervised task of rotation predictions by a multi-class minimax game. Although the proposed method is evaluated on different datasets, performance comparisons are made in lower resolution datasets where the higher resolution image generation is a more challenging problem.

Huang et al. [13] proposes an auxiliary task for the discriminator to predict whether the input image is unmodified or not. The modification is the feature exchanging on the feature maps attained from the hidden layer of the discriminator. It is stated that the discriminator performance improves for the discernment of structural inconsistencies in the images and the discriminator will feedback the generator to synthesize more structurally meaningful images. The authors claim that the pixel exchanging in the raw pixel space would push the discriminator to choose to learn low-level features instead of high-level features to distinguish the exchange. However, enhancing the discriminator to not only predict whether the pixel exchange is performed or not but also predict the order of the pixel block exchanges would lead to learning high-level features since the model should be capable of extracting these high-level features in order to capture the relative relationships of the patches. They also evaluate the incorporation of self-supervision tasks in conditional GANs yet, they do not evaluate the quality of the representations. Class-conditional training on ImageNet dataset can be used to evaluate the quality of the learnt representations by the discriminator.

In this work, we present a self-supervised GAN model, the DeshuffleGAN, that utilizes deshuffling task of jigsaw images in order to train a discriminator that learns high-level features through resolving the spatial configuration of the input data for generating structurally consistent images¹. We extend the DeshuffleGAN as follows:

- We compare the deshuffling task with the other self-supervision tasks deployed to the discriminator on various datasets as LSUN-Bedroom [15], LSUN-Church [15] and CelebA-HQ [16] in terms of generation quality.
- We study the effects of deshuffling auxiliary task on training through 2 different networks unconditionally. The first one consists of ResNet blocks as Miyato et al. [17] propose while the second one is designed based on DCGAN [18] architecture as Jolicoeur-Martineau proposes in [19] which makes use of relativistic adversarial training.
- We design the cDeshuffleGAN, the conditional version of the original model, and showcase the conditioned generation quality of the cDeshuffleGAN.
- We evaluate the representation quality of the features learnt by the cDeshuffleGAN on ImageNet dataset.
- We study the effects of self-supervision tasks on the loss landscape.

DeshuffleGAN surpasses the other self-supervision tasks in terms of generation quality which is evaluated with the Fréchet Inception Distance (FID) [20] measure whose reasonableness is empirically shown by Lucic et al. [21]. It improves the representation quality compared to the baseline architecture which is evaluated as Zhang et al. [22] proposed.

¹A preliminary version of our work is presented at IEEE International Conference on Image Processing 2020 [14].

2. Related Work

2.1. Self-Supervised Learning

Self-supervised learning is a two-staged method which is a subset of unsupervised learning and designed in order to learn qualified feature representations via training on unlabeled datasets. The first stage of the self-supervised learning is to use unlabeled datasets and label them with *pseudo-labels* which are produced automatically by manipulating the data in a way that the manipulation is not expensive besides its result is known already. Data with the pseudo-labels are used subsequently in a task called *pretext* which is designed for the DNN to solve with the purpose of learning visual features that encode high-level semantic information of the data. The second stage of self-supervised learning is to use the learnt visual features in other computer vision tasks called *downstream* tasks where the downstream tasks can be treated as the evaluation methods for the quality of the learnt features. The term “quality” indicates the representability and the generalizability of the features which is obviously desired for an efficient use in high-level problems.

The mostly used image-based pretext tasks can be categorized as *generation-based methods* which learn the features while generating images compatible with a data distribution, and *context-based methods* which learn the features while trying to capture context similarities or spatial context structures [23]. In generation-based methods such as Zhang et al. [22] where the task is the colorization of grey-scale images, the discriminator network learns the semantic features of the images and the learnt features by the discriminator can be beneficial for the downstream tasks. In context-based methods, a network is trained for a pretext task that can be designed for various context-related problems. Noroozi et al. [24] present a self-supervision task where the task is the prediction of shuffling order of the input image that is divided into 9 tiles like a jigsaw puzzle and shuffled with a random permutation which leads to learning spatial context structures of the images. Gidaris et al. [25] present the task of predicting the rotation angle of the input image where the input image might

be rotated from one of 4 different angles and the learning process gives results to obtain semantic information of the data such as object structures. Doersch et al. [26] introduce the task of finding the relationship between the positions of the two image patches which is managed by learning the high-level semantic information of the data.

Beyond the design of the pretext tasks, notable questions are answered such as the effects of the DNN choices for different pretext tasks by Kolesnikov et al. [27], the effects of employing multiple pretext tasks by Doersch et al. [28] and the usage of multiple-domain data by Feng et al. [29].

2.2. Generative Adversarial Networks

After the idea of two adversarial players is introduced by Goodfellow et al. [1], GANs received accelerating attention for the task of image generation. In order to satisfy the objectives of the image generation, various types of GANs are designed.

While some of the works try to overcome the problem of unconditional training instability by enforcing the discriminator to satisfy the Lipschitz condition [30, 31, 17, 32], other methods [33, 34, 35, 19] change the loss definitions which also aim to overcome the vanishing gradient problem of the generator or the mode collapse problem.

Various architectural designs are also proposed during the development of both unconditional and conditional GANs. DCGAN [18] proposes the usage of convolutions in GANs which results in the generation of higher resolution images. Progressive GANs [16] extend the network architecture progressively where the network includes millions of parameters and improves the generation quality while the training strategy improves stability. Self-Attention GANs [36] deploy the usage of attention mechanisms in order to learn global dependencies for generating images and to capture mode diversity with the help of a large receptive field. [36] is able to produce higher resolution images while ensuring to remedy the problem of vanishing gradients by deploying the spectral normalization to both the discriminator and the generator networks. BigGANs [37]

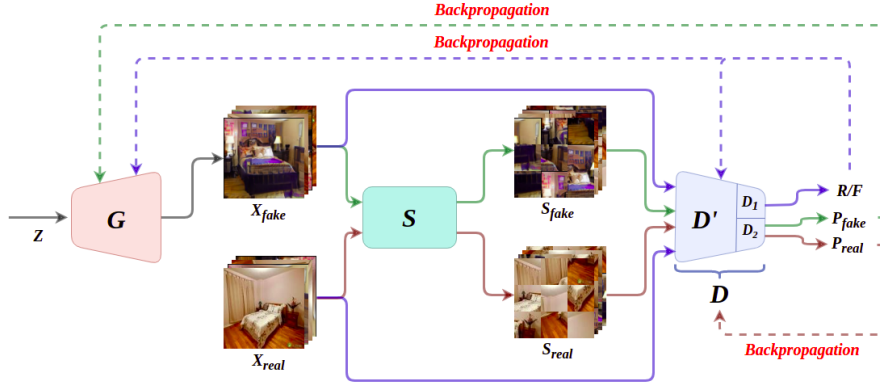


Figure 1: Proposed training mechanism for DeshuffleGAN. X_{fake} represents a batch of generated images while X_{real} represents the real images. S is the Shuffler and it shuffles X_{fake} and X_{real} as S_{fake} and S_{real} respectively. P_{fake} and P_{real} are the permutation predictions for S_{real} and S_{fake} . Green and Red lines indicate the shuffling and deshuffling operations, including their backpropagation paths. Purple lines refer to the standard adversarial training of the GAN.

introduce a deeper architecture that is based on the architecture of [36] and proposes to use very large batch sizes which require to have an enormous GPU power. [37] also deploys the attention mechanism and spectral normalization in order to obtain diversity in generations and to overcome the training stability problem.

3. Methodology

The proposed training mechanism for DeshuffleGAN is shown in Fig. 1. The standard adversarial training is visualized along with the auxiliary task training.

In the adversarial training, generator G takes a vector z which is sampled from the Gaussian normal distribution as $z \sim N(0, 1)$ with the size of 128×1 as input and learns to decode the latent space to the image space while the synthesized samples are named as X_{fake} . As the discriminator D learns to distinguish between the real samples and the fake samples, samples derived from the real data distribution are named as X_{real} and included to the adversarial training

of D along with X_{fake} . While D learns the discriminative features of the real data, it gives feedback to G that helps G in generating images compatible with the real data distribution. In classical adversarial training, the only feedback given to G from D is the prediction of whether the samples are real or fake.

In the training for the auxiliary self-supervision task, the main objective is to enrich the learnt features by D in a way to have well-defined structures that lead to the generation of structurally coherent and consistent images by G . To arrange the input data with pseudo-labels, a new component that is light in computation, which is obviously desired, is designed as the S block in Figure 1, denoting the *Shuffler* operation.

S is designed to divide its image inputs into 9 square tiles with the size of $n'/3$ and shuffle them with an order of permutation. n is the resized input image size and it may not be divisible by 3. Then, the biggest number smaller than n and divisible by 3 is obtained as n' and used to calculate the tile sizes. The generations in this work are 128×128 sized, so n' is used as 126 , and each image tile is obtained as a square with the size of 42×42 . The $n' \times n'$ sized top left area of the input image is used to construct a jigsaw puzzle of 3×3 in the shuffling process of S .

As there are 9 tiles, there are $9!$ possible permutations for shuffling, which is impractical to use. The number of permutations as in [38] is set to 30. The permutations are selected according to the Hamming distances proposed in [24]. Each sample in the input batch of S is shuffled by a different permutation out of 30, and the permutations applied to the input batch are selected randomly in order to prevent memorization. Since both X_{real} and X_{fake} play roles in the auxiliary task, they are shuffled by S to produce S_{real} and S_{fake} , respectively. To obtain the same input size n , S_{real} and S_{fake} are padded by 1 pixel on each side with a replication padding.

Originally, D has an output layer as the last stage of real/fake (r/f) prediction, which we name as D_1 . Since the cooperation of the auxiliary task needs an architectural enhancement on D , one additional output layer that learns to map the output of D' to permutation indices is added as D_2 . In DeshuffleGAN,

D' has the *same* shared weights for both of the tasks while D_1 layer outputs the r/f predictions for X_{real} and X_{fake} . D_2 layer outputs the permutation indices for S_{real} and S_{fake} . According to architectural design, output layers can be convolutional or linear.

DeshuffleGAN’s D is trained to capture the structural features within the input data by the deshuffling auxiliary task so that it can encourage G to generate structurally coherent images as D can deshuffle the shuffled versions of the generated images. As D is meant to learn structural features, it can easily deshuffle S_{fake} if X_{fake} is structurally consistent and includes meaningful pieces so that the puzzle tiles in S_{fake} are related to each other and obtain a continuity when they are deshuffled. On the contrary case of image generations that do not contain meaningfully structured elements, D signals G in a way to support it to synthesize well-structured and correctly composed images so that it can manage deshuffling S_{fake} .

The objectives for both adversarial and auxiliary training become more of an issue in that the choices for the objectives affect the performance of the model, therefore they need to be studied in detail.

3.1. Adversarial Objective

The standard GAN training proposed in [1] has distinct objectives for D and G , defined as:

$$\begin{aligned}
 L_\theta &= -\mathbb{E}_{x_r \sim P}[\log(D'(x_r))] - \mathbb{E}_{x_f \sim Q}[\log(1 - D'(x_f))] \\
 L_\phi &= -\mathbb{E}_{x_f \sim Q}[\log(D'(x_f))] \\
 D'(x_r) &= \textit{sigmoid}(D(x_r)) \\
 D'(x_f) &= \textit{sigmoid}(D(x_f))
 \end{aligned} \tag{1}$$

where x_r is the real data that is sampled from the real data distribution P , x_f is the generated data that is sampled from generated data distribution Q . θ and ϕ are the parameters of the D and G network models, respectively. $D(x)$

is the non-transformed output of D that measures the realness of the input x . In classical GAN training, cross-entropy loss is used as the error measure in Eq. (1). Sigmoid is the nonlinear transformation over the output of D in [1]. L_θ and L_ϕ refer to the objective functions for D and G , respectively.

Mao et al. [34] propose to disuse sigmoid as a transformation for the output of D in order to mitigate the vanishing gradient problem and modifies the adversarial objectives as:

$$\begin{aligned} L_\theta &= \frac{1}{2}\mathbb{E}_{x_r \sim P}[(D(x_r) - 1)^2] + \frac{1}{2}\mathbb{E}_{x_f \sim Q}[D(x_f)^2] \\ L_\phi &= \frac{1}{2}\mathbb{E}_{x_f \sim Q}[(D(x_f) - 1)^2]. \end{aligned} \quad (2)$$

Later, Lim et al. [35] show the geometrical nature of GANs, and [17] deploy the hinge loss to their GAN training as:

$$\begin{aligned} L_\theta &= -\mathbb{E}_{x_r \sim P}[\min(0, -1 + D(x_r))] \\ &\quad -\mathbb{E}_{x_f \sim Q}[\min(0, -1 - D(x_f))] \\ L_\phi &= -\mathbb{E}_{x_f \sim Q}[D(x_f)]. \end{aligned} \quad (3)$$

Even if the formulations change according to different concerns such as stability and optimality, in all of the training mechanisms shown with Eq. (1) - (3), D returns a probabilistic result for the input being real as G tries to boost the probability of the fake data being real. Relativistic GANs [19] argue that D should converge to 0.5 in order to maximize the JS-divergence between X_{real} and X_{fake} while the classical adversarial training actually causes D to output 1 for all data. It is also shown that when D is optimal, its gradients mostly come from the fake samples. Therefore, D later cannot learn from the real images. As a solution, the “relativism” idea is introduced in [19], as the aim of the GAN training should be not only to increase the probability that the fake data are real, but also to decrease the probability that the real data are real. That means the realness of the input is not considered separately but

considered relatively. Then the relativism idea is further enhanced to define a more global D as the author says, in a way that the average $D(x)$ results for the random samples of opposing type are used in the calculations and the objectives integrate “relativistic average” idea.

The relativistic average objective used in this work deploys the relativism idea into the least squares objective formulized in Eq. (2) as:

$$\begin{aligned}
 L_\theta &= \frac{1}{2} \mathbb{E}_{x_r \sim P} [(D(x_r) - \mathbb{E}_{x_f \sim Q} D(x_f) - 1)^2] \\
 &\quad + \frac{1}{2} \mathbb{E}_{x_f \sim Q} [(D(x_f) - \mathbb{E}_{x_r \sim P} D(x_r))^2] \\
 L_\phi &= \frac{1}{2} \mathbb{E}_{x_r \sim P} [(D(x_r) - \mathbb{E}_{x_f \sim Q} D(x_f) + 1)^2] \\
 &\quad + \frac{1}{2} \mathbb{E}_{x_f \sim Q} [(D(x_f) - \mathbb{E}_{x_r \sim P} D(x_r) - 1)^2]
 \end{aligned} \tag{4}$$

As numerous GAN models exist, we evaluate the performances of two different GAN architectures as the backbone in our self-supervised DeshuffleGAN. We utilize the hinge loss objective formulated in Eq. (3) for the modified GAN architecture proposed in [17], named as SNGAN. We utilize the relativistic average least squares objective (RaLSGAN) formulated in Eq. (4) for the DCGAN [18] architecture as in [19]. We add one more linear layer to the discriminator of the SNGAN architecture, and one convolutional layer to the discriminator of the DCGAN architecture as D_2 for the deshuffling task as in Figure 1.

As the adversarial training concerns only X_{real} and X_{fake} for the r/f predictions, S_{real} and S_{fake} are not included in the adversarial objectives.

3.2. The Deshuffler Objective

Besides the adversarial objectives, DeshuffleGAN involves additional objectives for D and G in order to increase the learning capability of D by deshuffling the shuffled images in order to improve the quality of the generation that is produced by G .

For D , the objective is to correctly predict the shuffling order of S_{real} , meaning that the difference between P_{real} (permutation predictions for S_{real}) and the

true random permutations used by S to shuffle X_{real} should be minimized. As D should learn solely the features of the real data, it should be updated in a way to minimize the error calculated only considering S_{real} . Cooperation of S_{fake} to the optimization of D would lead to a problem of learning fake and unnecessary features of the generated data hence G would not be supported to synthesize images that are compatible to the real data distribution. The cross-entropy loss is used as the deshuffler optimization objective for D :

$$V_{\theta} = - \sum_n^N y_d^n \ln \tilde{y}_d^n \quad (5)$$

where N denotes the number of samples in an input batch, y_d^n is the one-hot encoded label vector of size 30×1 applied to the n^{th} sample of X_{real} and \tilde{y}_d^n is the n^{th} permutation prediction vector of P_{real} . θ are the parameters of the D network.

For G , the objective is to generate high quality images X_{fake} for which D can correctly predict the shuffling order of S_{fake} . Therefore, the error between P_{fake} and the random permutations used by S to shuffle X_{fake} is desired to be a minimum. As D learns the features of the real data, if S_{fake} can be deshuffled by D , G can be expected to generate images compatible to the real data distribution. On the other hand, if the generations are not structurally consistent and do not capture the features of the real data, then D which learns the features of the real data cannot deshuffle S_{fake} , thus sends a signal to G to synthesize qualified images so that it can deshuffle S_{fake} . The cross-entropy loss is used as the deshuffler optimization objective for G :

$$V_{\phi} = - \sum_n^N y_g^n \ln \tilde{y}_g^n \quad (6)$$

where N denotes the number of samples in an input batch, y_g^n is the one-hot encoded label vector of size 30×1 applied to the n^{th} sample of X_{fake} and \tilde{y}_g^n is the n^{th} permutation prediction vector of P_{fake} . ϕ are the parameters of the G network.

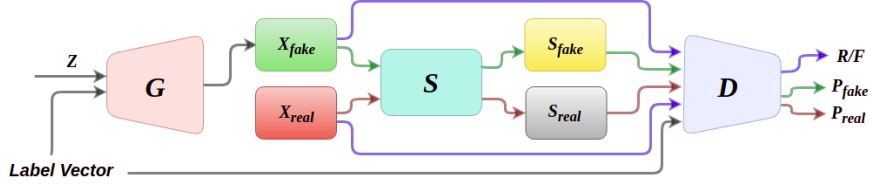


Figure 2: Proposed model for cDeshuffleGAN. The training mechanism is the same as the DeshuffleGAN while the cDeshuffleGAN is also supported with the class label.

3.3. Full Objective of the DeshuffleGAN

We formulate the full objective as the combination of the adversarial objective and the deshuffler objective as follows:

$$\begin{aligned} L_{\theta}^D &= L_{\theta} + \alpha V_{\theta} \\ L_{\phi}^G &= L_{\phi} + \beta V_{\phi} \end{aligned} \quad (7)$$

where α and β parameters determine the influence of the objectives in the overall training. In our experiments, α is selected as 1 and the choice for β is made according to the experimental results as in [10] and determined as 0.5.

The training of the DeshuffleGAN model involves optimization of the objective functions L_{θ}^D and L_{ϕ}^G with respect to θ and ϕ parameters, respectively for the D and the G networks as follows:

$$\begin{aligned} \theta &= \arg \min L_{\theta}^D \\ \phi &= \arg \min L_{\phi}^G. \end{aligned} \quad (8)$$

3.4. cDeshuffleGAN

As an extension to the proposed DeshuffleGAN, we also train a conditional DeshuffleGAN, which we call cDeshuffleGAN. Fig. 2 shows the proposed model

of the cDeshuffleGAN. We utilize the conditional SNGAN in [17], cSNGAN, as the baseline architecture for cDeshuffleGAN. The main difference between the DeshuffleGAN and the cDeshuffleGAN is the utilization of the label vector in the training. The main training objective for the cDeshuffleGAN is to evaluate the representation quality learnt by D on the ImageNet dataset. Therefore, we enhance the capacity of the SNGAN which is relatively a smaller network with not only the auxiliary self-supervision signal but also with the class label in order to obtain meaningful generated samples of ImageNet. By doing so, we perform quantitative evaluations of representation quality learnt by the cSNGAN and cDeshuffleGAN.

4. Experiments

4.1. Experimental Settings

In our work, we show the effects of deshuffling self-supervision on GAN training using various datasets and GAN architectures.

As the datasets, we choose LSUN-Bedroom, CelebA-HQ, and LSUN-Church to compare the self-supervision tasks deployed to GANs and to analyze the effects of the self-supervision on GANs in terms of losses. We also use ImageNet in order to evaluate the representation quality of the features.

We utilize two distinct adversarial objectives for different backbones: (i) we experiment with the relativistic loss on the RaLSGAN which is based on the DCGAN [18] architecture; (ii) we experiment with hinge-loss on the modified version of the SNGAN architecture where we use the proposed channel sizes by Kurach et al. [39] for the D and the G . As the reduced channel sizes were empirically reported to improve the performance in [39], we also utilize these small differences which simplify the architecture design in our implementation. For ImageNet experiments, we employ the conditional SNGAN as the baseline and deploy deshuffling unit over its architecture. We use the same modified channel sizes for the conditional SNGAN and modify the G and D architectures for conditioning as in [17].



Figure 3: Randomly generated samples for (a) LSUN-Bedroom and (b) LSUN-Church by the best-performing DeshuffleGANs.

We use Adam optimizer [40] for the RaLSGAN D and G with $(0.5, 0.999)$ parameters, and for the SNGAN D and G with $(0, 0.9)$ parameters, respectively. Learning rate is set to 0.0002, and batch size is set to 64 for all experiments. We choose the number of total iterations as 200K for the LSUN-Bedroom, CelebA-HQ, and LSUN-Church while we perform 1M iterations on ImageNet. We select the number of D iterations per G as 1 and 2 for the RaLSGAN, and the SNGAN, respectively. We conduct all of the experiments on a single V100 GPU. We use the PyTorch framework for the implementations.

4.2. Evaluations

4.2.1. Generation Quality

Visual results for the LSUN-Bedroom and the LSUN-Church are shown in Fig 3. In order to numerically evaluate the generation quality of the DeshuffleGANs on different datasets, we use the most generally preferred evaluation metric FID [20], and compare our method with the other methods. FID compares the statistical metrics of the real data distribution and the generated data distribution where the lower difference between the measurements indicate

Table 1: Best FID results obtained for each dataset.

DATASET	METHOD	FID
LSUN-Church	SS-GAN	33.82
	FX-GAN	-
	SNGAN	22.17
	SNGAN + Deshuffle	14.01
	RaLSGAN	22.02
	RaLSGAN + Deshuffle	21.47
LSUN-Bedroom	SS-GAN [10]	13.30
	FX-GAN [13]	12.90
	SNGAN	51.22
	SNGAN + Deshuffle	10.13
	RaLSGAN	34.76
	RaLSGAN + Deshuffle	36.48
CelebA-HQ	SS-GAN [10]	24.36
	FX-GAN [13]	19.25
	SNGAN	20.55
	SNGAN + Deshuffle	32.46
	RaLSGAN	25.29
	RaLSGAN + Deshuffle	22.51

more similarity between the distributions, which is obviously the desired case. A comparison between the methods on the datasets are given in Table 1. From the literature, we report the best FID values that are obtained for the LSUN-Bedroom and CelebA-HQ datasets for the SS-GAN from [10] and the FX-GAN from [13]. For the LSUN-Church dataset, we run the official implementation of [10]. As the official implementation of the FX-GAN [13] is not published, we do not report the values of the FX-GAN for the LSUN-Church dataset. FID curves of all the methods compared in Table 1 are shown in Fig 4.

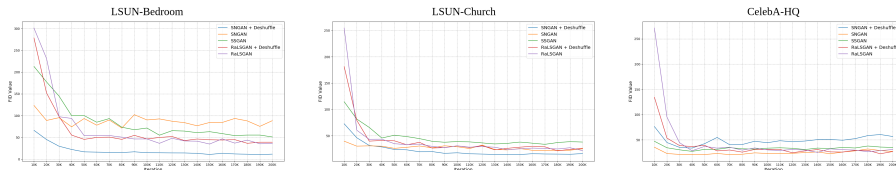


Figure 4: FID curves for each of the datasets. For LSUN datasets, the DeshuffleGANs achieve the best performances and the training stability of the DeshuffleGANs reflects the smoothness of the FID curves.

In Fig 5, we present class-conditional generations of ImageNet by the conditional DeshuffleGAN. The motivation for the ImageNet training is to evaluate the quality of the representations by a commonly used method where the main objective is not to generate high-quality images conditionally which is only manageable with massive networks and enormous computational power. Nonetheless, we manage to generate visually substantial samples with a relatively smaller network and computational power than the successful networks like BigGANs [37].

4.2.2. Representation Quality

In order to test whether the learnt representations of the D are meaningful or not, we use a commonly preferred evaluation method proposed in [22], which basically suggests training a linear layer on the representations that are extracted from the hidden layers of D and use the trained layer for the classification task on ImageNet. For the representation quality evaluation, we use conditional SNGAN. The D of the SNGAN consists of 6 ResNet blocks and we extract the representations of the last block which is the 6th block as they represent the high-level features.

In Fig. 6, we show that the linear layer trained on the representations extracted from the conditional DeshuffleGAN performs better than the linear layer trained on the representations extracted from the original conditional SNGAN on ImageNet test data. These results provide evidence to our hypothesis that the learnt features of the DeshuffleGAN model increases the effectiveness of the

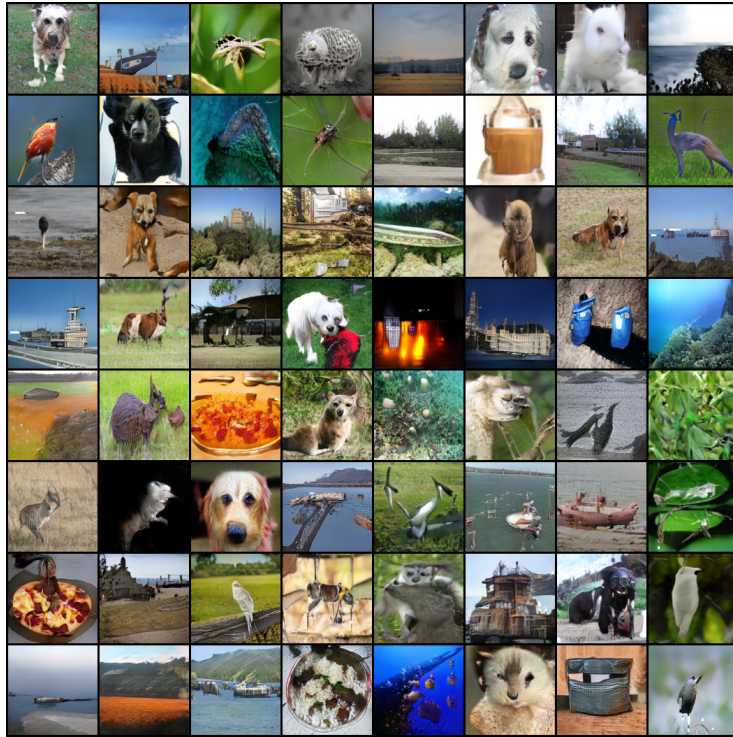


Figure 5: Randomly generated samples for ImageNet by the conditional DeshuffleGAN.

representation power of a baseline GAN model, here exemplified by the original SNGAN.

4.3. Discussion

We show that the modified architecture of SNGAN with the addition of deshuffling task outperforms other methods and achieves better performances on LSUN-Bedroom and LSUN-Church datasets in terms of both numerical and visual results as the Table 1 and Fig. 3 indicate, respectively.

When the deshuffling is deployed to the baseline settings, we observe that the deshuffling improves the performance of the SNGAN for considerable amounts on LSUN datasets while it improves the performance of RaLSGAN on LSUN-Church and CelebA-HQ datasets. We also observe that the deshuffling increases or decreases the performance of the RaLSGAN in small amounts. This may be

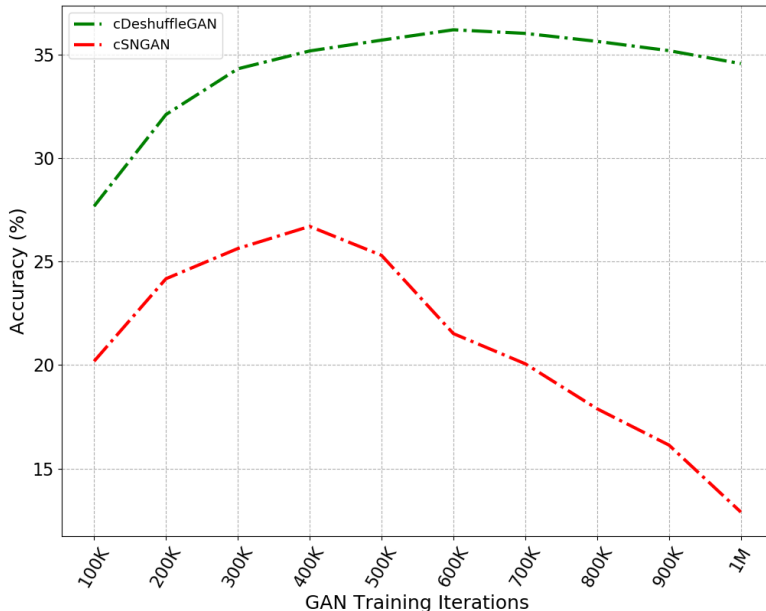


Figure 6: Top-1 accuracies of the regressors trained on the final layer representations of the discriminators attained at each 100K iterations.

because the RaLSGAN setting is already stabilized and its capacity to solve the problems is enough. As the architectural designs for the RaLSGAN which is based on the DCGAN and the SNGAN differ, we can state that the design of the D matters such that the capacity of the D to solve the additional tasks and its availability for the enhancements affect how much the self-supervision task can help towards an improved learning.

Apart from the LSUN datasets, CelebA-HQ is the only dataset that the deshuffling self-supervision seems to be not cooperative to improve the learning for the SNGAN setting. [10] also shows that the rotation prediction self-supervision cannot get ahead of the SNGAN.

CelebA-HQ has a certain structural space based on the faces of humans, that is constrained in a specific way. This indicates that the complexity of the underlying data distribution is less than that of the environments in the LSUN

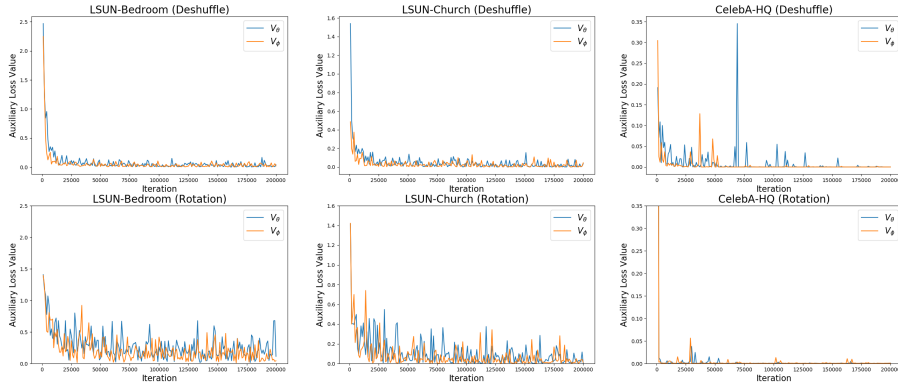


Figure 7: The deshuffler loss values of SNGAN + Deshuffle and SS-GAN settings for all datasets. Self-supervision tasks seem to be non-cooperative for the learning process.

data spaces. Therefore, we conjecture that the reason for both self-supervision tasks, namely the deshuffling and rotation prediction, to be not supportive of the learning features of CelebA-HQ are due to the semantics of the dataset.

Apart from the semantics of the datasets, we also study the self-supervision losses over different datasets and observe that the speed for learning to deshuffle actually matters. As Fig 7 shows, the auxiliary deshuffling losses V_θ and V_ϕ of the D and the G respectively for both rotation prediction and deshuffling tasks on CelebA-HQ dataset start nearly at 0 and do not seem to improve. These results for both the deshuffling and rotation predictions tasks indicate that actually, these self-supervision tasks are not effective enough on the loss landscape during the training. On the other hand, the loss curves of the deshuffling task on LSUN-Bedroom and LSUN-Church datasets seem to be cooperative on learning. Compared to the rotation prediction task, the loss curves of the deshuffling for LSUN-Bedroom and LSUN-Church datasets seem more stabilized and smoother.

The most important contribution of the self-supervision framework for the GAN training is that the self-supervised GANs are shown to alleviate the catastrophic forgetting problem [10]. Catastrophic forgetting problem arises from the non-stationary nature of the GAN training. In an unconditional setting, D tends to forget the earlier tasks, and self-supervision is shown to help to avoid

this problem in [10].

When we evaluate the representation quality of the learnt features for both the conditional DeshuffleGAN and the conditional SNGAN, we also demonstrate that the enhancement of the D by the deshuffling task alleviates the catastrophic forgetting in Fig. 6, as the D of the conditional SNGAN seems to forget the useful information after the 400K iterations while the D of the conditional DeshuffleGAN seems to carry the information during the GAN training. Therefore, we can state that the DeshuffleGANs improve the training stability so that they can better address the catastrophic forgetting problem than their baseline counterparts.

5. Conclusion

In this work, we present the DeshuffleGAN and the cDeshuffleGAN that incorporate the deshuffling task, which is previously used only as a pretext in self-supervised learning, into the GAN framework. This incorporation increases the discriminator’s representation power through improved structure learning.

Compared to the baseline versions, the visual inspection shows particularly that a more consistent generation quality is obtained by DeshuffleGANs because they struggle to put the pieces of an unshuffled image together while trying to generate realistic outputs, and this pushes them to learn improved features to represent the global spatial structure and appearance of the input data space as well as its local structural continuity and coherence.

We show that DeshuffleGANs can improve the performance of different GAN architectures which indicate the generalizability of the deshuffling task. We also use various datasets for the generations in order to prove the capability of DeshuffleGANs over different data distributions. DeshuffleGANs can manage to generate images with complex representations such as buildings, human faces, or bedrooms. However, we show that the performance of the DeshuffleGAN varies with respect to the complexity of the underlying data distribution. Within more complex environments such as the LSUN data spaces, the DeshuffleGAN

demonstrates its well-enhancing effects, whereas, for more constrained structural spaces such as the faces of humans, its effect is inconsequential.

Furthermore, we compare the deshuffling task with the rotation prediction task. We show that for most of the settings and via FID curves, the deshuffling task aids the adversarial training more than the rotation task. We hypothesize that the reason is due to the relatively higher complexity of the deshuffling task compared to that of the rotation prediction task. As the discriminator learns to solve a more complex structural problem in deshuffling, the discriminator gets further enhanced compared to the rotation prediction, which is only a global transformation problem.

As future work, the reasons why the deshuffling task does not improve the baseline performance on some datasets can be analyzed deeply. In this work, we show the non-cooperative behavior of the auxiliary tasks for CelebA-HQ dataset on the loss landscape. However, there remains open questions on what kind of and how auxiliary signals should be incorporated within various settings.

Acknowledgment

In this work, Gulcin Baykal and Furkan Ozcelik were supported by the Turkcell-ITU Researcher Funding Program. This work was also supported by the Scientific Research Project Unit of Istanbul Technical University [project number MOA-2019-42321].

References

References

- [1] I. Goodfellow, J. Pouget-Abadie, M. Mirza, B. Xu, D. Warde-Farley, S. Ozair, A. Courville, Y. Bengio, Generative adversarial nets, in: NIPS, 2014.
- [2] H. Bourlard, Y. Kamp, Auto-association by multilayer perceptrons and singular value decomposition, *Biol. Cybern.* 59 (4-5) (1988) 291–294.

- [3] Z. Wang, Q. She, T. E. Ward, Generative adversarial networks: A survey and taxonomy, ArXiv abs/1906.01529.
- [4] M. Mirza, S. Osindero, Conditional generative adversarial nets, ArXiv abs/1411.1784.
- [5] T. Miyato, M. Koyama, cGANs with projection discriminator, in: International Conference on Learning Representations, 2018.
- [6] X. Chen, Y. Duan, R. Houthoofd, J. Schulman, I. Sutskever, P. Abbeel, Infogan: Interpretable representation learning by information maximizing generative adversarial nets, in: NIPS, 2016.
- [7] A. Odena, C. Olah, J. Shlens, Conditional image synthesis with auxiliary classifier gans, in: ICML'17, 2017.
- [8] J. Deng, W. Dong, R. Socher, L.-J. Li, K. Li, L. Fei-Fei, ImageNet: A Large-Scale Hierarchical Image Database, in: CVPR09, 2009.
- [9] A. Krizhevsky, Learning multiple layers of features from tiny images, Tech. rep. (2009).
- [10] T. Chen, X. Zhai, M. Ritter, M. Lucic, N. Houlsby, Self-supervised gans via auxiliary rotation loss, in: CVPR, 2019, pp. 12154–12163. doi:10.1109/CVPR.2019.01243.
- [11] J. Kirkpatrick, R. Pascanu, N. Rabinowitz, J. Veness, G. Desjardins, A. A. Rusu, K. Milan, J. Quan, T. Ramalho, A. Grabska-Barwinska, et al., Overcoming catastrophic forgetting in neural networks, Proceedings of the national academy of sciences 114 (13) (2017) 3521–3526.
- [12] N.-T. Tran, V.-H. Tran, N.-B. Nguyen, L. Yang, N.-M. Cheung, Self-supervised gan: Analysis and improvement with multi-class minimax game, in: NeurIPS, 2019.
- [13] R. Huang, W. Xu, T.-Y. Lee, A. Cherian, Y. Wang, T. K. Marks, Fx-gan: Self-supervised gan learning via feature exchange, 2020 IEEE Winter

- Conference on Applications of Computer Vision (WACV) (2020) 3183–3191.
- [14] G. Baykal, G. Unal, DeshuffleGAN: A self-supervised gan to improve structure learning, in: 2020 IEEE International Conference on Image Processing (ICIP), 2020, pp. 708–712.
 - [15] F. Yu, Y. Zhang, S. Song, A. Seff, J. Xiao, Lsun: Construction of a large-scale image dataset using deep learning with humans in the loop, arXiv preprint arXiv:1506.03365.
 - [16] T. Karras, T. Aila, S. Laine, J. Lehtinen, Progressive growing of GANs for improved quality, stability, and variation, in: International Conference on Learning Representations, 2018.
 - [17] T. Miyato, T. Kataoka, M. Koyama, Y. Yoshida, Spectral normalization for generative adversarial networks, in: International Conference on Learning Representations, 2018.
 - [18] A. Radford, L. Metz, S. Chintala, Unsupervised representation learning with deep convolutional generative adversarial networks (2015). [arXiv:1511.06434](#).
 - [19] A. Jolicoeur-Martineau, The relativistic discriminator: a key element missing from standard gan, in: International Conference on Learning Representations, 2019.
 - [20] M. Heusel, H. Ramsauer, T. Unterthiner, B. Nessler, S. Hochreiter, Gans trained by a two time-scale update rule converge to a local nash equilibrium, in: NIPS, 2017, p. 6629–6640.
 - [21] M. Lucic, K. Kurach, M. Michalski, O. Bousquet, S. Gelly, Are gans created equal? a large-scale study, in: Proceedings of the 32nd International Conference on Neural Information Processing Systems, 2018, p. 698–707.

- [22] R. Zhang, P. Isola, A. A. Efros, Colorful image colorization, in: ECCV, 2016.
- [23] L. Jing, Y. Tian, Self-supervised visual feature learning with deep neural networks: A survey, IEEE transactions on pattern analysis and machine intelligence.
- [24] M. Noroozi, P. Favaro, Unsupervised learning of visual representations by solving jigsaw puzzles, in: ECCV, 2016.
- [25] S. Gidaris, P. Singh, N. Komodakis, Unsupervised representation learning by predicting image rotations, in: International Conference on Learning Representations, 2018.
- [26] C. Doersch, A. Gupta, A. A. Efros, Unsupervised visual representation learning by context prediction, 2015 IEEE International Conference on Computer Vision (ICCV) (2015) 1422–1430.
- [27] A. Kolesnikov, X. Zhai, L. Beyer, Revisiting self-supervised visual representation learning, 2019 IEEE/CVF Conference on Computer Vision and Pattern Recognition (CVPR) (2019) 1920–1929.
- [28] C. Doersch, A. Zisserman, Multi-task self-supervised visual learning, 2017 IEEE International Conference on Computer Vision (ICCV) (2017) 2070–2079.
- [29] Z. Feng, C. Xu, D. Tao, Self-supervised representation learning from multi-domain data, 2019 IEEE/CVF International Conference on Computer Vision (ICCV) (2019) 3244–3254.
- [30] M. Arjovsky, L. Bottou, Towards principled methods for training generative adversarial networks, ArXiv abs/1701.04862.
- [31] I. Gulrajani, F. Ahmed, M. Arjovsky, V. Dumoulin, A. C. Courville, Improved training of wasserstein gans, in: Advances in neural information processing systems, 2017, pp. 5767–5777.

- [32] Z. Zhang, Y. Zeng, L. Bai, Y. Hu, M. Wu, S. Wang, E. R. Hancock, Spectral bounding: Strictly satisfying the 1-lipschitz property for generative adversarial networks, *Pattern Recognition* 105 (2020) 107179.
- [33] M. Arjovsky, S. Chintala, L. Bottou, Wasserstein gan, in: *International Conference on Machine Learning*, 2017, pp. 214–223.
- [34] X. Mao, Q. Li, H. Xie, R. Y. K. Lau, Z. Wang, S. P. Smolley, Least squares generative adversarial networks, *ICCV* (2016) 2813–2821.
- [35] J. H. Lim, J. C. Ye, Geometric gan (2017). [arXiv:1705.02894](https://arxiv.org/abs/1705.02894).
- [36] H. Zhang, I. J. Goodfellow, D. N. Metaxas, A. Odena, Self-attention generative adversarial networks, in: *International Conference on Machine Learning*, 2019, pp. 7354–7363.
- [37] A. Brock, J. Donahue, K. Simonyan, Large scale GAN training for high fidelity natural image synthesis, in: *International Conference on Learning Representations*, 2019.
- [38] F. M. Carlucci, A. D’Innocente, S. Bucci, B. Caputo, T. Tommasi, Domain generalization by solving jigsaw puzzles, in: *Proceedings of the IEEE Conference on Computer Vision and Pattern Recognition*, 2019, pp. 2229–2238.
- [39] K. Kurach, M. Lučić, X. Zhai, M. Michalski, S. Gelly, A large-scale study on regularization and normalization in GANs, Vol. 97 of *Proceedings of Machine Learning Research*, PMLR, 2019, pp. 3581–3590.
- [40] D. P. Kingma, J. Ba, Adam: A method for stochastic optimization (2014). [arXiv:1412.6980](https://arxiv.org/abs/1412.6980).



Gulcin Baykal received her B.Sc. and M.Sc. degrees of Computer Engineering from Istanbul Technical University (ITU) in 2018 and 2020, respectively. Gulcin is currently pursuing her Ph.D. as an ITU-DeepMind scholar in Computer Engineering at ITU. Her main research interests focus on representation learning, deep learning and generative

models.



Furkan Ozcelik received his B.Sc. and M.Sc. degrees of Computer Engineering from Istanbul Technical University (ITU) in 2018 and 2020, respectively. His main research interests focus on deep learning, representation learning and generative models.



Gozde Unal is a professor of Computer Engineering at Istanbul Technical University (ITU). She is the founder of ITU-AI Center. She is the recipient of the Marie Curie Alumni Association (MCAA) Career Award 2016 of European Commission. Her main research interests are in computer vision

and deep learning, particularly representation learning and generative models.